

Pressure-induced ferroelastic transition and internal displacement in TeO₂

Hiromoto Uwe and Hiroshi Tokumoto

Electrotechnical Laboratory, Tanashi, Tokyo, Japan

(Received 13 September 1978)

The soft effective elastic constant $C_s = \frac{1}{2}(C_{11} - C_{12})$ of TeO₂ has been measured at 77 K as functions of the uniaxial-stress loads in the [110], $[\bar{1}10]$, and [001] directions up to 4 kbar. By using the method of Thurston and Brugger, we have determined the values of the third-order elastic constants as $C_{111} - C_{122} = 3.85$ and $C_{113} - C_{123} = -0.39$ in 10^{12} dyn/cm². These values are not big in comparison with those of other materials. The origin of the pressure-induced ferroelastic transition found by Percy and Fritz can be attributed to the anomalously small elastic constant C_s at 1 bar as well as the negative pressure coefficient of C_s . For the purpose of evaluation of the elastic constant, by making use of a model lattice with two-dimensional covalent bondings, we have calculated Keating's strain energy which includes the homogeneous strain and the internal displacement as variables. An internal displacement of oxygen atoms, which corresponds to the spontaneous internal displacement previously found by Worlton and Beyerlein in the high-pressure ferroelastic phase, is found concurrently to follow the homogeneous strain $e_{xx} - e_{yy}$ so as to suppress the increase of an O-Te-O bond-bending energy: This leads to the result $C_{11} - C_{12} = 0$. The pressure dependence of the spontaneous internal displacements and the supralinear changes of the A_1 - and B_1 -optical-phonon frequencies under the [100] uniaxial pressure are interpreted by using Landau's free energy which includes the interaction terms between the homogeneous strain and the internal displacements, and the parameters in the free-energy are determined.

I. INTRODUCTION

Paratellurite (TeO₂) has the anomalously small elastic constant $C_s = \frac{1}{2}(C_{11} - C_{12})$. Percy and Fritz¹ found that the effective elastic constant C_s decreases with the hydrostatic pressure to vanish at a critical pressure p_c . The temperature dependence of p_c was found small.² In this pressure-induced phase transition of the second-order type, characteristics expected from Landau's phenomenological theory were observed: The square of the spontaneous strain was found to develop in proportion to $p - p_c$,^{3,4} and the soft elastic constants above and below p_c change linearly with pressure.² We call this phase transition the pressure-induced ferroelastic phase transition. Neutron scattering experiments⁴ showed that the softening of the corresponding acoustic mode is restricted to the $q \rightarrow 0$ limit in the Brillouin zone. An optical-phonon instability was not observed by Raman scattering measurements.² Neutron-powder-diffraction measurements,³ however, gave microscopic information that the oxygen atoms undergo large internal displacements in going through the transition. In this point, we can find a phenomenological resemblance to the case of the phase transition of Nb₃Sn,⁵ in which a sublattice displacement of Γ_{12}

(+) type takes place, without optical-phonon instability, through bilinear coupling with the spontaneous strain.

The purpose of the present paper is to give a lattice-dynamical interpretation of the pressure-induced ferroelastic phase transition in TeO₂. This phase transition might take place due to the following properties of TeO₂: (a) the initial elastic constant at 1 bar is anomalously small, and (b) the pressure coefficient of the shear elastic constant is negative. Furthermore, the symmetry of the crystal allows the transition to be continuous.² From the data of Ref. 2 ($\Delta C_{11}/\Delta p = 5.2$, $\Delta C_{33}/\Delta p = 13.5$, $\Delta C_{44}/\Delta p = -1.1$, $\Delta C_{66}/\Delta p = 7.1$, $\Delta C_s/\Delta p = -2.6$), we find that the magnitude of the pressure coefficient $\Delta C_s/\Delta p$ is not large in comparison with that of other components of the elastic constant. The values of the third-order elastic constants, which are components of the hydrostatic-pressure coefficient of C_s , will be estimated in Sec. II by means of a uniaxial-pressure experiment and found not large in comparison with other materials. Thus, we find that the (a) property is important. The (b) property is not peculiar to TeO₂; several materials (for example, rubidium halides, KCl, and zinc-blende-structure crystals such as CuCl and ZnTe) exhibit this behavior.⁶ Thus, in

this paper, we will consider, in Sec. III, the reason why the elastic constant is small even at zero pressure; and the Keating's method⁷ for the evaluation of the elastic constant will be applied to a model lattice. The relation between the soft homogeneous strain $e_{xx} - e_{yy}$ and the internal displacement of the oxygen atoms will also be found. In Sec. IV, the pressure dependence of the internal displacement and the optical-phonon behavior under uniaxial pressure⁸ will be considered in the light of the phenomenological free energy, which is analogous to that of Nb₃Sn and corresponds to the Keating's strain energy.

II. UNIAXIAL-PRESSURE EFFECT ON THE SOFT ACOUSTIC MODE

We measured the velocity of the acoustic shear mode in the $[\bar{1}10]$ direction with $[110]$ polarization as a function of the uniaxial stress in the $[110]$, $[\bar{1}10]$, and $[001]$ directions. Single crystals of TeO₂ were oriented by x rays to have (110) , $(\bar{1}10)$, and (001) faces. Typical dimensions of the sample were $2.5 \times 2.5 \times 5$ mm³; the compressional stress was applied along the longest length. The stress apparatus was the same as the one used for the dielectric and Raman measurements⁹; the sample and the pressing blocks were directly immersed in liquid nitrogen.

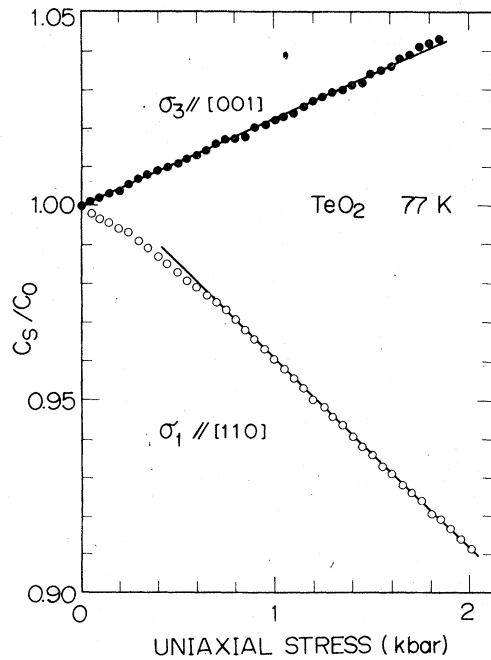


FIG. 1. Change of the effective elastic constant $C_s = \frac{1}{2}(C_{11} - C_{12})$ as a function of the uniaxial-stress load σ_1 ($//[110]$) or σ_3 ($//[001]$) (both perpendicular to the ultrasonic-propagation direction $[\bar{1}10]$).

The magnitude of the applied stress was measured by the calibrated strain gauge in a load cell. For the excitation of the transverse acoustic mode we used a Y-cut quartz transducer (15 MHz). When the ultrasonic propagation direction ($[\bar{1}10]$) was perpendicular to the uniaxial stress axis ($[110]$ or $[001]$), the transducer, as small as $(1.5)^2$ mm², was bonded with indium metal and the round-trip time was measured by the standard pulse-echo-overlap technique^{10,11} by using a Metec 950 unit. When the ultrasonic wave was propagated along the stress axis, the transducer was sandwiched between the specimen and the pressing block, and Nonaq-stop-cock grease was padded between the sample and the transducer. In this case, pulse-echo traces on the oscilloscope changed their shapes irregularly at each stress load, possibly because of the inhomogeneous region of strain near the pressing blocks; then, we measured directly the time intervals between pulse echoes on the oscilloscope.

Figures 1 and 2 show the uniaxial-pressure (σ_i) dependence of the elastic constant C_s , normalized by the free-stress value C_0 , which was deduced from the ultrasonic velocity. For the stress direction ($[110]$ (σ_1) or $[001]$ (σ_3)) perpendicular to the ultrasonic-propagation direction ($[\bar{1}10]$), C_s changes linearly in a wide pressure range, as shown in Fig. 1. In Fig. 2 for the case of the $[\bar{1}10]$ stress (σ_2), experimental points scatter, since the pulse-echo-overlap technique could not be used, as mentioned above. Thurston and Brugger^{12,13} gave a general expression for the pressure coefficient of the elastic constant for arbitrary crystal symmetry. On direct application of the result¹² to Fig. 1, we get for stress along $[110]$,

$$\begin{aligned} \frac{1}{C_0} \frac{\Delta C_s}{\Delta \sigma_1} &= -s^2 C_{33} - \frac{1}{2C_{66}} - \frac{s^2}{4C_0} \\ &\quad \times [(C_{111} - C_{112})C_{33} - 2(C_{113} - C_{123})C_{13}] \\ &= -4.92 \times 10^{-11} \text{ cm}^2/\text{dyn}, \end{aligned} \quad (1)$$

and for stress along $[001]$,

$$\begin{aligned} \frac{1}{C_0} \frac{\Delta C_s}{\Delta \sigma_3} &= 2s^2 C_{13} + \frac{s^2}{2C_0} [(C_{111} - C_{112})C_{13} \\ &\quad - (C_{113} - C_{123})(C_{11} + C_{12})] \\ &= 2.24 \times 10^{-11} \text{ cm}^2/\text{dyn}. \end{aligned} \quad (2)$$

From Eqs. (1) and (2), we get the following values:

$$\begin{aligned} C_{111} - C_{112} &= 3.85 \times 10^{12} \text{ dyn/cm}^2, \\ C_{113} - C_{123} &= -0.39 \times 10^{12} \text{ dyn/cm}^2, \end{aligned} \quad (3)$$

where the $C_{\lambda\mu}$ values of Ohmachi and Uchida¹⁴ (150–390 K) are extrapolated to liquid-nitrogen temperature

$$\begin{aligned} C_{11} &= 5.96, & C_{12} &= 5.59, & C_{13} &= 1.50, \\ C_{33} &= 11.14, & C_{44} &= 2.71, & C_{66} &= 7.32, \\ C_0 &= 0.186 \text{ in } 10^{11} \text{ dyn/cm}^2, \end{aligned}$$

and

$$\begin{aligned} s^2 &\equiv [(C_{11} + C_{12})C_{33} - 2C_{13}^2]^{-1} \\ &= 8.05 \times 10^{-25} \text{ cm}^4/\text{dyn}^2. \end{aligned}$$

The values of Eqs. (3) may contain an experimental error of 15% due to the error in the $C_{\lambda\mu}$ values at 77 K.

For stress along $[\bar{1}10]$, on application of the formula of Ref. 11,

$$\begin{aligned} \frac{1}{C_0} \frac{\Delta C_s}{\Delta \sigma_2} &= \frac{1}{C_0} \frac{\Delta C_s}{\Delta \sigma_1} + \frac{1}{C_{66}} - \frac{1}{C_0} \\ &= -10.2 \times 10^{-11} \text{ cm}^2/\text{dyn}. \end{aligned} \quad (4)$$

In Fig. 2 the predicted values of Eq. (4) are shown by a broken line which agrees fairly well with the experimental results.

For the case of hydrostatic pressure, we get from Eqs. (1), (2), and (4),¹⁵

$$\begin{aligned} \frac{1}{C_0} \frac{\Delta C_s}{\Delta p} &= \frac{1}{C_0} \left(\frac{\Delta C_s}{\Delta \sigma_1} + \frac{\Delta C_s}{\Delta \sigma_2} + \frac{\Delta C_s}{\Delta \sigma_3} \right) \\ &= -12.9 \times 10^{-11} \text{ cm}^2/\text{dyn}. \end{aligned} \quad (5)$$

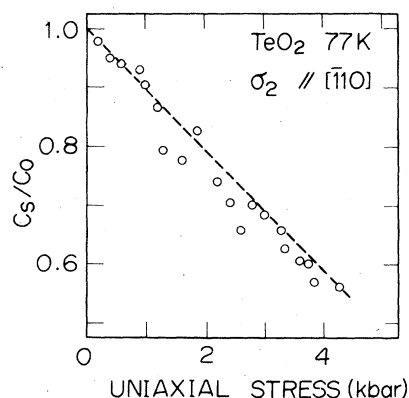


FIG. 2. Change of C_s as a function of uniaxial-stress load σ_2 (parallel to the ultrasonic-propagation direction $[\bar{1}10]$). The broken line is drawn by the theory in the text and the data in Fig. 1.

Then, the elastic constant goes to zero at a pressure corresponding to the inverse of Eq. (5), $p_c = 7.8 \times 10^9 \text{ dyn/cm}^2$, which agrees with the previously reported values² (7.76 or $7.84 \times 10^9 \text{ dyn/cm}^2$ at 75.6 K)

The third-order elastic constant of Eq. (3) are found to be only one order of magnitude larger than the second-order ones except for C_0 . The absolute values of these constants are also rather common to other normal materials; for example, $C_{111} = -8.2 \times 10^{12} \text{ dyn/cm}^2$ for Si,¹⁶ and $-9.7 \times 10^{12} \text{ dyn/cm}^2$ for NaCl.¹⁷ Thus, it is concluded that the pressure-induced ferroelastic phase transition is ascribed to the anomalously small elastic constant $C_s = \frac{1}{2}(C_{11} - C_{12})$ at 1 bar and the negative pressure coefficient of C_s .

III. DISCUSSION OF THE SMALL ELASTIC CONSTANT

Figure 3 shows the crystal structure which was determined by using the neutron-diffraction method.¹⁸ We can find the strongly distorted square pyramids of TeO_4 , which are linked with the common oxygen atoms to form the three-dimensional lattice. The structure could be regarded as covalent, because (a) the distances between Te and O are equal to covalent bond lengths,¹⁸ (b) the directions of the bonds are highly anisotropic,¹⁸ and (c) the refractive index is large, so that the effective charge is small.² Thus the stiffness of the crystal might be determined mainly by the short-range bond-to-bond interaction.

Worlton and Beyerlein³ found that the oxygen atoms undergo large internal displacements in going through the pressure-induced phase transition, as shown in Fig. 3(b). The Te-atoms displacements are small. It is noted that the O-atoms displacements are nearly perpendicular to the collinear bond vectors, for example, x_{II} and x_{III} , which link Te_I to $\text{O}_{(\text{I})}$ and Te_II to $\text{O}_{(\text{I})}$, respectively. This internal displacement might take place in order to avoid the hard bond bending or the hard bond stretching due to the spontaneous homogeneous strain $e_{xx} - e_{yy}$. With the Keating's method⁷ for calculating the elastic constant of the covalent-bond crystal, it is easy to see the relation between the homogeneous strain and the internal displacement. The real TeO_2 lattice is too complex to apply the method straightforwardly. So we take a simple two-dimensional model lattice (Fig. 4), in which the O atoms link the Te atoms to the other Te atoms collinearly with different bond lengths a and b whereas the bond angles around the Te atoms are taken as 90° . Here, we assume that the Te atoms do not have internal displacements, since the Te atom is heavy compared to the O atom. By taking up to the nearest-neighbor bond-to-bond in-

teractions, the strain energy U is

$$\begin{aligned}
 U = & \frac{\alpha_1}{a^2} [(\bar{x}_{11}^2 - a^2)^2 + (\bar{x}_{13}^2 - a^2)^2 + (\bar{x}_{112}^2 - a^2)^2 + (\bar{x}_{V4}^2 - a^2)^2] \\
 & + \frac{\alpha_2}{b^2} [(\bar{x}_{12}^2 - b^2)^2 + (\bar{x}_{14}^2 - b^2)^2 + (\bar{x}_{111}^2 - b^2)^2 + (\bar{x}_{V3}^2 - b^2)^2] \\
 & + \frac{\beta_1}{ab} [(\bar{x}_{11} \cdot \bar{x}_{111} + ab)^2 + (\bar{x}_{14} \cdot \bar{x}_{V4} + ab)^2 + (\bar{x}_{13} \cdot \bar{x}_{V3} + ab)^2 + (\bar{x}_{12} \cdot \bar{x}_{112} + ab)^2] \\
 & + \frac{\beta_2}{ab} [(\bar{x}_{11} \cdot \bar{x}_{12})^2 + (\bar{x}_{12} \cdot \bar{x}_{13})^2 + (\bar{x}_{13} \cdot \bar{x}_{14})^2 + (\bar{x}_{14} \cdot \bar{x}_{11})^2 \\
 & + (\bar{x}_{111} \cdot \bar{x}_{115})^2 + (\bar{x}_{115} \cdot \bar{x}_{116})^2 + (\bar{x}_{116} \cdot \bar{x}_{117})^2 + (\bar{x}_{117} \cdot \bar{x}_{111})^2], \quad (6)
 \end{aligned}$$

where α_1 , α_2 , β_1 , and β_2 correspond to the force constants. The \bar{x} 's are the bond vectors which link Te to O, and they can be expressed by the homogeneous strains e_{xx} , e_{yy} , e_{xy} , and the internal displacements of the O atoms, u_i , v_i , w_i ,

$$\begin{aligned}
 (\bar{x}_{13})_x &= \frac{a}{2^{1/2}} (1 + e_{xx} + \frac{1}{2} e_{xy}) + u_3, \\
 (x_{13})_y &= \frac{a}{2^{1/2}} (1 + e_{xx} + \frac{1}{2} e_{xy}) + v_3, \quad \text{etc.} \quad (7)
 \end{aligned}$$

The internal displacements can also be expressed by the following normal coordinates Q_1, Q_2, \dots, Q_8 . We have

$$\begin{pmatrix} Q_1 \\ Q_2 \\ Q_3 \\ Q_4 \end{pmatrix} = \frac{1}{2} \begin{pmatrix} 1 & 1 & 1 & 1 \\ 1 & -1 & 1 & -1 \\ 1 & 1 & -1 & -1 \\ 1 & -1 & -1 & 1 \end{pmatrix} \begin{pmatrix} u_1 + v_1 \\ u_2 - v_2 \\ -u_3 - v_3 \\ -u_4 + v_4 \end{pmatrix}, \quad \begin{pmatrix} Q_5 \\ Q_6 \\ Q_7 \\ Q_8 \end{pmatrix} = \frac{1}{2} \begin{pmatrix} 1 & 1 & 1 & 1 \\ 1 & -1 & 1 & -1 \\ 1 & 1 & -1 & -1 \\ 1 & -1 & -1 & 1 \end{pmatrix} \begin{pmatrix} u_1 - v_1 \\ -u_2 - v_2 \\ -u_3 + v_3 \\ u_4 + v_4 \end{pmatrix}. \quad (8)$$

From Eqs. (6), (7), and (8), we get

$$\begin{aligned}
 U = & C[(e_{xx} + e_{yy})^2 + e_{xy}^2] + K_1[L_1(e_{xx} - e_{yy}) + Q_6]^2 + K_2\{[Q_1 - L_2(e_{xx} + e_{yy})]^2 + (Q_2 - L_2 e_{xy})^2 + Q_3^2 + Q_4^2\} \\
 & + K_3 Q_5^2 + K_4(Q_7^2 + Q_8^2), \quad (9)
 \end{aligned}$$

where

$$\begin{aligned}
 C &= \frac{[\alpha_1 \alpha_2 (a+b)^2 + \beta_1 (\alpha_1 a^4 + \alpha_2 b^4) / ab]}{[\alpha_1 a^2 + \alpha_2 b^2 + \beta_1 (a-b)^2 / ab]}, \\
 K_1 &= \frac{\beta_2 (a-b)^2}{ab}, \quad K_2 = 2 \left[\frac{\alpha_1 + \alpha_2 + \beta_1 (a-b)^2}{ab} \right], \\
 K_3 &= \frac{\beta_2 (a+b)^2}{ab}, \quad K_4 = \frac{\beta_2 (a^2 + b^2)}{ab}, \quad L_1 = \frac{8^{1/2} ab}{(a-b)}, \\
 L_2 &= \frac{2^{1/2} [\alpha_1 a - \alpha_2 b - \beta_1 (a-b)]}{[\alpha_1 + \alpha_2 + \beta_1 (a-b)^2 / ab]}. \quad (10)
 \end{aligned}$$

K_1, K_2, \dots, K_4 denote the force constants for the internal displacements Q_i in the clamped state, and thus correspond to the optical-phonon frequencies. The energy in Eq. (9) takes a minimum value when

$$\begin{aligned}
 Q_1 &= L_2(e_{xx} + e_{yy}), \quad Q_2 = L_2 e_{xy}, \\
 Q_6 &= -L_1(e_{xx} - e_{yy}), \quad Q_3 = Q_4 = Q_5 = Q_7 = Q_8 = 0.
 \end{aligned}$$

Substitution of these Q_i values into Eq. (9) yields the elastic energy ϕ ,

$$\phi = C[(e_{xx} + e_{yy})^2 + e_{xy}^2]. \quad (11)$$

Therefore, according to the definition of elastic constant,

$$C_{11} - C_{12} = 0, \quad C_{11} = C_{66} = 2C. \quad (12)$$

The experimental values for the elastic constants are $C_{11} = 5.6$, $C_{12} = 5.1$, and $C_{66} = 6.6$ in 10^{11} dyn/cm² at room temperature¹⁴; thus Eqs. (12) are well satisfied. We find, in Eq. (9), that the strain energy due to $e_{xx} - e_{yy}$ vanishes owing to the internal displacement Q_6 ; this leads to the result $C_{11} - C_{12} = 0$. The displacement Q_6 shown by arrows in Fig. 4 is found to correspond well to the internal displacement in the real TeO₂ [Fig. 3(b)], which follows as a result of the development of the spontaneous strain. Thus, the model lattice might well represent the elastic properties of TeO₂ in the c plane.

The displacement Q_6 does not change the right O-Te-O bond angles, but alters the collinear Te-O-Te bond angles. The collinear bonds are easy to bend, because, in Eq. (6), the displacement Q_6 perpendicular to the collinear bond vectors such as \bar{x}_{III} and \bar{x}_{II} does not affect the value of the scalar product between the bond vectors. If the equilibrium

Te-O-Te bond angles deviate from 180° , as in the real lattice, additional bilinear coupling between $e_{xx} - e_{yy}$ and Q_6 might come in from the interaction of the third term in Eq. (6), so that the renormalized $C_{11} - C_{12}$ becomes finite.

IV. PHENOMENOLOGICAL DISCUSSION

In this section we will interpret the following facts phenomenologically on the basis of Sec. III: (a) The internal displacement in the high-pressure phase³ includes the total symmetric one (Q_{A_1}) in addition to the B_1 symmetric one (Q_{B_1} , same symmetry as the strain $e_{xx} - e_{yy}$), which corresponds to Q_6 in Sec. III, and (b) the A_1 - or B_1 - symmetry optical phonon exhibits a supralinear frequency change under [100] uniaxial stress.⁸

From symmetry considerations, the Helmholtz's free energy per unit volume, F , can be expanded with the homogeneous strain $e = e_{xx} - e_{yy}$ and the internal displacements or optical-phonon amplitudes Q_{A_1} and Q_{B_1} ,

$$F = \frac{1}{2}Ce^2 + \frac{1}{2}AQ_{A_1}^2 + \frac{1}{3}A'Q_{A_1}^3 + \frac{1}{2}BQ_{B_1}^2 + \frac{1}{4}B'Q_{B_1}^4 - DeQ_{B_1} - Ee^2Q_{A_1} + \dots \quad (13)$$

By minimizing F with respect to Q_i , we have

$$Q_{A_1} = (E/A)e^2, \quad Q_{B_1} = (D/B)e. \quad (14)$$

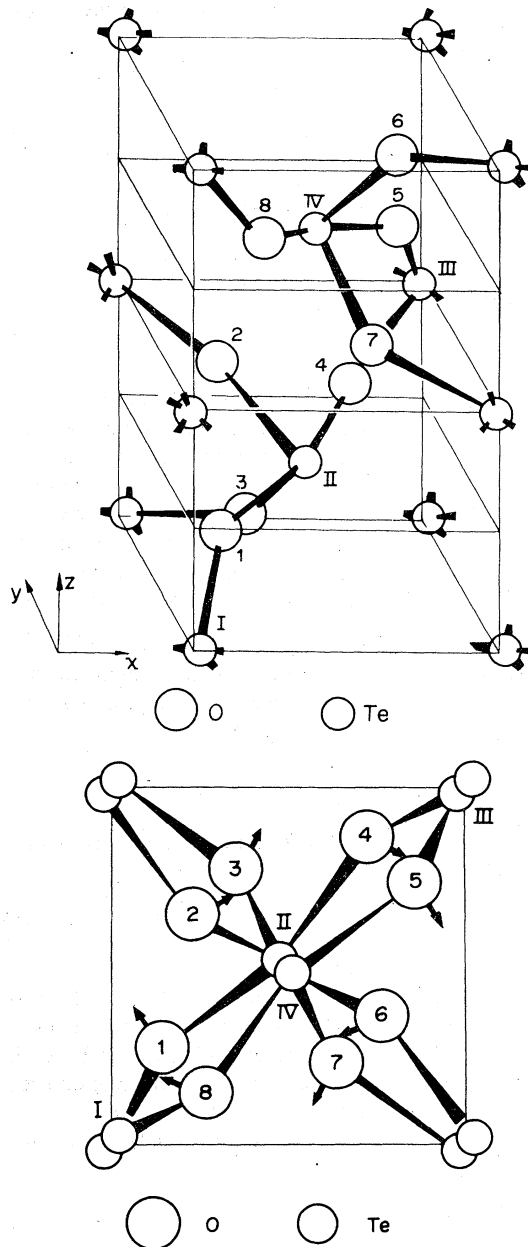


FIG. 3. (a) Crystal structure of TeO₂. The strongly distorted square pyramids TeO₄ are linked with the common oxygen atoms. (b) Internal displacement of the oxygen atoms projected on the c plane, which follows the spontaneous strain $e_{xx} - e_{yy}$ in the high-pressure phase.

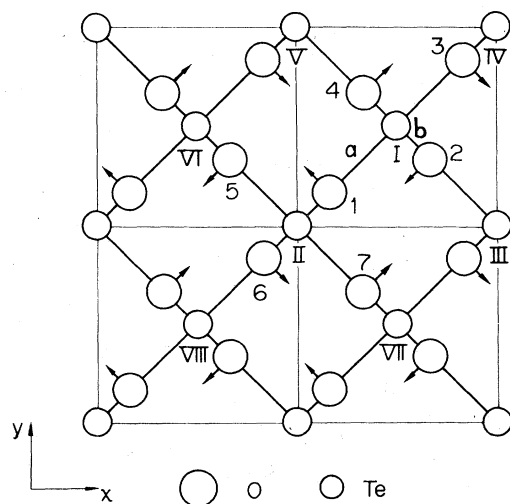


FIG. 4. Two-dimensional model lattice for estimating the elastic constants. The internal displacement Q_6 is shown by the arrows.

TABLE I. Parameters of the free energy [Eq. (13) in the text] in cgs units.

A	A'	B	B'	D	E	C	M_0
9.43×10^{26}	$(1.78 \pm 0.44) \times 10^{34}$	1.61×10^{26}	$(2.06 \pm 0.24) \times 10^{42}$	$(5.51 \pm 0.31) \times 10^{18}$	$(1.79 \pm 0.44) \times 10^{20}$	$(2.12 \pm 0.21) \times 10^{11}$	1.21

Substitution of Eq. (14) into Eq. (13) yields the elastic Gibbs energy, from which the elastic constant is deduced,

$$\frac{1}{2}(C_{11} - C_{12}) = C - D^2/B. \quad (15)$$

This value is anomalously small, as was discussed in Sec. III by using the model lattice.

In going through the pressure-induced ferroelastic phase transition, the development of the spontaneous strain $e = e_s$ yields the internal displacements according to Eq. (14). It is noted here that these internal displacements are not accompanied by precursors, as in the case of Nb_3Sn ,⁵ since they take place owing to the improper effect; thus, in the Raman experiment,² the unstable optical phonon was not observed. The increase of the Debye-Waller factor³ for oxygen atoms near p_c (the maximum value is at ~ 4 kbar above p_c) should be attributed to effects other than

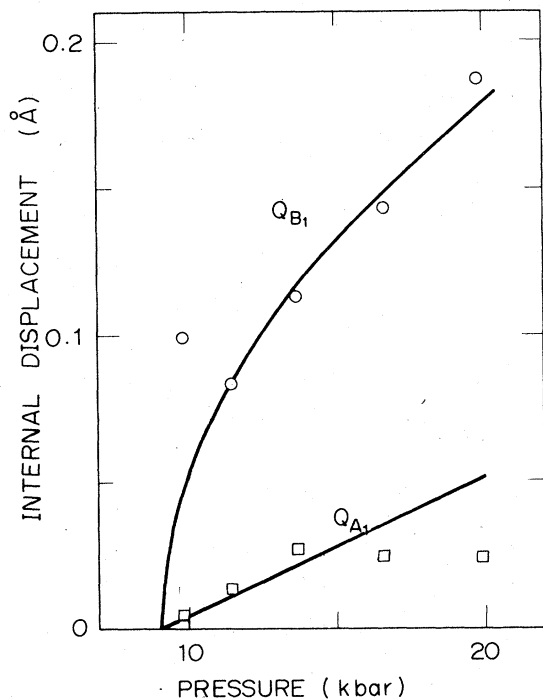


FIG. 5. Hydrostatic-pressure dependence of the internal displacements Q_{A_1} and Q_{B_1} which are estimated from the data in Ref. 3. The full lines are from the phenomenological theory in the text.

the optical-phonon instability. Let us evaluate the Q_{A_1} and Q_{B_1} from data of Ref. 3 by the following expressions¹⁹:

$$\begin{aligned} Q_{A_1}^2 &= \left\{ \left[\frac{1}{2}(x_3 - \frac{1}{4} + y_2) - y \right]^2 \right. \\ &\quad + \left[\frac{1}{2}(y_3 + \frac{1}{4} + x_2) - x - \frac{1}{4} \right]^2 \bigg\} a^2 \\ &\quad + \left[\frac{1}{2}(-z_3 + \frac{1}{4} + z_2) - z - \frac{1}{8} \right]^2 c^2, \\ Q_{B_1}^2 &= \left[\frac{1}{4}(x_3 - \frac{1}{4} - y_2)^2 + \frac{1}{4}(y_3 + \frac{1}{4} - x_2)^2 \right] a^2 \\ &\quad + \frac{1}{4}(z_3 - \frac{1}{4} + z_2)^2 c^2, \end{aligned} \quad (16)$$

where x_2, y_2, z_2, x_3, y_3 , and z_3 are the fractional-atomic-position coordinates of the oxygen atoms in the high-pressure D_2^4 phase defined in Ref. 3, and x, y, z are the ones from the low-pressure D_4^4 phase, and $a = 4.80 \text{ \AA}$ and $c = 7.6 \text{ \AA}$ are the lattice parameters. Here we neglect the small displacement of the Te atoms. Figure 5 shows the pressure dependence of Q_{A_1} and Q_{B_1} . We can find the proportionality between Q_{B_1} and e_s in agreement with Eq. (14), since e_s varies as $(p - p_c)^{1/2}$. Because of the smallness of Q_{A_1} , the pressure dependence of Q_{A_1} is not clear in the figure. By using the result³

$$e_s^2 = 2.53 \times 10^{-4} p - 2.30 \times 10^{-3}$$

(p in kbar) and Fig. 5, the values of parameters in Eq. (14) are

$$D/B = 3.42 \pm 0.19 \text{ \AA}, \quad E/A = 19.0 \pm 4.7 \text{ \AA}. \quad (17)$$

Next, Lemos *et al.* found that the A_1 and B_1 optical phonons exhibit supralinear frequency changes under [100] uniaxial pressure: This result can be obtained from Eq. (13) too. Under [100] uniaxial pressure X , we can assume that the strain $e = e_{xx} - e_{yy}$ dominates, since $C_{11} - C_{12}$ is anomalously small; we have

$$e = \frac{X}{C_{11} - C_{12}}. \quad (18)$$

The internal displacements Q_{A_1} and Q_{B_1} are induced according to Eq. (14) at this time. Other displacements do not appear, since they do not couple with the strain. The optical-phonon frequencies ω_{A_1} and

ω_{B_1} are given by the following equations⁹:

$$M_0\omega_{A_1}^2 = \left. \frac{\partial^2 F}{\partial Q_{A_1}^2} \right|_{\text{eq}}, \quad M_0\omega_{B_1}^2 = \left. \frac{\partial^2 F}{\partial Q_{B_1}^2} \right|_{\text{eq}}, \quad (19)$$

where the derivatives should be taken at the equilibrium state, and $M_0 = 8m_0/v$ is the mass density of the oxygen atoms (v is the unit-cell volume). Due to the presence of the higher-order terms in the free energy of Eq. (13), one obtains the uniaxial-pressure change of ω_i ; we get, from Eqs. (13), (14), (18), and (19),

$$\omega_{\delta A_1}^2 = \frac{A}{M_0}, \quad \omega_{\delta B_1}^2 = \frac{B}{M_0}, \quad (20)$$

$$\omega_{A_1}^2 = \omega_{\delta A_1}^2 + \frac{2A'E}{M_0A(C_{11}-C_{12})^2}X^2, \quad (21)$$

$$\omega_{B_1}^2 = \omega_{\delta B_1}^2 + \frac{3B'D^2}{M_0B^2(C_{11}-C_{12})^2}X^2,$$

Thus, we have

$$\Delta\omega_{A_1}/\Delta X^2 = A'E/M_0^2(C_{11}-C_{12})^2\omega_{\delta A_1}^3,$$

and

$$\Delta\omega_{B_1}/\Delta X^2 = 3B'D^2/2M_0^3(C_{11}-C_{12})^2\omega_{\delta B_1}^5.$$

These quadratic stress changes of ω should be added to the result of the linear-deformation-potential theory.⁸ From the ω_{0i} dependence, these coefficients are found to be large only for the lowest-frequency optical phonons, in agreement with observation.⁸ When comparing the above results with the experimental ones⁸

$$\omega_{0A_1} = 148.1 \text{ cm}^{-1}, \quad \Delta\omega_{A_1}/\Delta X^2 = 0.24 \text{ cm}^{-1} \text{ kbar}^{-2},$$

$$\omega_{0B_1} = 61.1 \text{ cm}^{-1}, \quad \Delta\omega_{B_1}/\Delta X^2 = 0.66 \text{ cm}^{-1} \text{ kbar}^{-2},$$

we get

$$A = 9.43 \times 10^{26}, \quad B = 1.61 \times 10^{26},$$

$$A' = (1.78 \pm 0.44) \times 10^{34}, \quad B' = (2.06 \pm 0.24) \times 10^{42}$$

in cgs units, where we used $M_0 = 1.210 \text{ g/cm}^3$ and the results of Eq. (17). Combining these with the results of Eqs. (15) and (17), all of the parameters in the free energy of Eq. (13) are yielded as listed in Table I.

V. SUMMARY

For the TeO_2 single crystal, the pressure dependence of the soft effective elastic constant $C_s = \frac{1}{2}(C_{11}-C_{12})$ has been analyzed by the higher-order elasticity theory, and some of the third-order elastic constants were determined. It was found that, because C_s is anomalously small initially at 1 bar and the pressure coefficient of C_s is negative, a pressure-induced ferroelastic phase transition takes place: The pressure coefficient of the elastic constant is not large.²⁰ By using a model crystal of TeO_2 , the reason for the small elastic constant is explained: It was found that an internal displacement follows concurrently the homogeneous strain $e_{xx}-e_{yy}$ to cancel the strain energy, so that $C_{11}-C_{12} \approx 0$. This internal displacement corresponds to the rotational oxygen-atom displacement in the high-pressure phase which was found by Worlton and Beyerlein.³ By using the Landau theory of the phase transition, we could interpret the pressure dependence of the internal displacement and the supralinear change of the optical-phonon frequency under [100] uniaxial pressure.⁸

ACKNOWLEDGMENTS

We are much indebted to A. Watanabe and T. Yano of Matsushita Research Institute for supplying us with excellent-quality crystals of TeO_2 . We wish to thank T. Sakudo for helpful discussions, encouragement, and support during our study, and T. Ishiguro, H. Unoki, Y. Fujii, and K. Oka for valuable discussions and help with the experiment.

¹P. S. Peercy and I. J. Fritz, Phys. Rev. Lett. **32**, 466 (1974).

²P. S. Peercy, I. J. Fritz, and G. A. Samara, J. Phys. Chem. Solids **36**, 1105 (1975).

³T. G. Worlton and R. A. Beyerlein, Phys. Rev. B **12**, 1899 (1975).

⁴D. B. McWhan, R. J. Birgeneau, W. A. Bonner, H. Taub, and J. D. Axe, J. Phys. C **8**, L81 (1975).

⁵G. Shirane and J. D. Axe, Phys. Rev. B **4**, 2957 (1971).

⁶For rubidium halides, Z. P. Chang and G. R. Barsch, J.

Phys. Chem. Solids **32**, 27 (1971); for KCl, D. Lazarus, Phys. Rev. **76**, 545 (1949); for zinc-blende-structure crystals, R. C. Hanson, K. Helliwell, and C. Schwab, Phys. Rev. B **9**, 2649 (1974) and references therein.

⁷P. N. Keating, Phys. Rev. **145**, 637 (1966).

⁸V. Lemos, F. Cerdeira, M. A. F. Scarparo, and R. S. Katiyar, Phys. Rev. B **16**, 5560 (1977).

⁹H. Uwe and T. Sakudo, Phys. Rev. B **13**, 271 (1976).

¹⁰E. P. Papadakis, J. Acoust. Soc. Am. **42**, 1045 (1967).

¹¹D. H. Chung, D. J. Silversmith, and B. B. Chick, *Rev. Sci. Instr.* **40**, 718 (1969).

¹²R. N. Thurston and K. Brugger, *Phys. Rev.* **133**, A1604 (1964).

¹³See also D. C. Wallace, in *Solid State Physics*, edited by H. Ehrenreich, F. Seitz, and D. Turnbull, (Academic, New York, 1970), Vol. 25, p. 301.

¹⁴Y. Ohmachi and N. Uchida, *J. Appl. Phys.* **41**, 2307 (1970).

¹⁵Equation (5) leads to the expression, $C_5 = (\alpha + \beta)(p_c - p)$, where $\alpha = 1 + s^2(C_{11} - C_{12})(C_{33} - C_{13})$, and

$$\beta = \frac{1}{2}s^2[(C_{33} - C_{13})(C_{111} - C_{112}) + (C_{11} + C_{12} - 2C_{13})(C_{113} - C_{123})].$$

In the theory of Ref. 4, α is absent. The elastic energy in the higher-order-elasticity theory should be expanded with the Lagrangian strains and also by using the conjugate thermodynamic stresses; this introduces α [H. Uwe (unpublished)]. In Fritz and Peercy's theory [I. J. Fritz and P. S. Peercy, *Solid State Commun.* **16**, 1197 (1975), and also Ref. 3], the elastic constant itself is assumed pressure dependent, not in accordance with the elastic-constant definition of the present paper and Refs. 12 and 13.

¹⁶H. J. McSkimin and P. Andreatch, Jr., *J. Appl. Phys.* **35**, 3312 (1964).

¹⁷J. R. Drabble and R. E. B. Strathen, *Proc. Phys. Soc. London* **92**, 1090 (1967).

¹⁸J. Leciejewicz, *Z. Kristallogr. Kristallgeom. Krystallphys. Kristallchem.* **116**, S.345 (1961).

¹⁹The derivation of Eq. (16) is as follows; let us consider the z component of the oxygen-atom displacement in Fig. 3(b). For oxygen 1, for example, the displacement is the sum of the A_1 -type one z_{A_1} and the B_1 -type one $z_{B_1}(z_{A_1} + z_{B_1})$. By the fourfold screw rotation of the D_4^4 phase, the oxygen 1 goes to the position of the oxygen 2, and thus, the displacement of the oxygen 2 should be $z_{A_1} - z_{B_1}$; on the other hand, since the displacements of the oxygens 1 and 2 are expressed as $z_2 - z - \frac{1}{8}$ and $(-z_3 + \frac{1}{4}) - z - \frac{1}{8}$, respectively, by using the notation of Ref. 3; we get z_{A_1} and z_{B_1} corresponding to the last terms in Eqs. (16). Similarly, taking into account the x and y components of the displacements, we get Eq. (16).

²⁰Recently, Jorgensen *et al.* [J. D. Jorgensen, T. G. Worlton, and J. C. Jamieson, *Phys. Rev. B* **17**, 2212 (1978)] found that NiF_2 undergoes a pressure-induced phase transition at 18.3 kbar. Above the transition pressure, the spontaneous strain $e_{xx} - e_{yy}$ was found to develop, and also the spontaneous B_{1g} rotational displacement of the F atoms was found. These findings are similar to the case of TeO_2 ; however, the pressure dependence of the elastic constant was suggested to be nonlinear [J. P. Jorgensen *et al.*, *ibid.*; and A. Y. Wu, *Phys. Lett. A* **60**, 260 (1977)] and the possibility was pointed out that the B_{1g} -optical-phonon instability may be related to the transition.